Overview of Full-Dimension MIMO in LTE-Advanced Pro

Hyoungju Ji[*+], Younsun Kim[*] and Juho Lee[*]
Eko Onggosanusi[†], Younghan Nam[†] and Jianzhong Zhang[†]
Byungju Lee[‡]
Byonghyo Shim[+]
[*]*Samsung Electronics Seoul R&D Center,* [†]*Samsung Research America, Dallas,*
[‡]*Purdue University, and* [+]*Seoul National University*

Abstract

Multiple-input multiple-output (MIMO) systems with large number of basestation antennas, often called massive MIMO systems, have received much attention in academia and industry as a means to improve the spectral efficiency, energy efficiency, and processing complexity. Mobile communication industry has initiated a feasibility study to meet the increasing demand of future wireless systems. Field trials of the proof-of-concept systems have demonstrated the potential gain of the Full-Dimension MIMO (FD-MIMO) and 3rd generation partnership project (3GPP) standard body has initiated the standardization activity for the seamless integration of this technology into current 4G LTE systems. A study item, process done before a formal standardization process, has been completed in June 2015 and the follow up work item process will be finalized shortly for the formal standardization of Release 13. In this article, we provide an overview of the FD-MIMO system, with emphasis on the discussion and debate conducted on standardization process of Release 13. We present key features for FD-MIMO systems, summary of the major issues for the standardization and practical system design, and performance evaluation for typical FD-MIMO scenarios.

I. Introduction

Multiple-input multiple-output (MIMO) systems with large number of basestation antennas, often referred to as *massive MIMO systems*, have received much attention in academia and industry as a means to improve the spectral efficiency, energy efficiency, and also processing complexity [1]. The wisdom behind the massive MIMO systems is that when the number of

basestation antennas goes to infinity, multiuser interference caused by the downlink user co-scheduling and uplink multiple access approaches to zero, resulting in a dramatic increase in the throughput with relative simple transmitter and receiver operations. While the massive MIMO technology is one of key enabler for the next generation cellular systems, there are many practical challenges down the road to the successful commercialization. These include design of low-cost and low-power basestation with acceptable antenna space, improvement in the fronthaul capacity between radio and control units, acquisition of high dimensional channel state information (CSI), and many others. Recently, 3rd generation partnership project (3GPP) standard body initiated the standardization activity for the massive MIMO systems with an aim to satisfy the spectral efficiency requirement of future cellular systems [2], [3]. Considering the implementation cost and complexity, and also the timeline to the real deployment, standard body decided to use tens of antennas with two dimensional (2D) array structure as a starting point. Full-Dimension MIMO (FD-MIMO), an official name for massive MIMO for 3GPP, targets the system utilizing up to 64 antenna ports at the transmitter side. Recently, field trials of the proof-of-concept FD-MIMO systems have been conducted successfully [4]. A study item, process done before a formal standardization process, has been completed in June 2015 and the follow up work item process will be finalized soon for the formal standardization of Release 13.[1]

The purpose of this article is to provide an overview of the FD-MIMO systems with an emphasis on the discussion and debate conducted on standardization process of Release 13. We note that preliminary studies addressed feasibility of 2D array antenna structure and performance evaluation in ideal scenarios (non-precoded CSI-RS and ideal feedback) [2], [3]. This work is distinct from previous efforts in the sense that we put out emphasis on key features for standardization such as (TXRU architectures, beamformed CSI-RS, 3D beamforming), details of CSI feedback issues, and performance evaluation in realistic FD-MIMO scenarios with new feedback schemes.

II. Key Features of FD-MIMO Systems

In this section, we discuss key features of FD-MIMO systems. These include large number of basestation antennas, two dimensional active antenna array, 3D channel propagation, and new pilot transmission with CSI feedback. In what follows, we will use LTE terminology exclusively:

[1]LTE-Advanced Pro is the LTE marker that is used for the specifications from Release 13 onwards by 3GPP.

enhanced node-B (eNB) for basestation, user equipment (UE) for the mobile terminal, and reference signal (RS) for pilot signal.

A. Increase the number of transmit antennas

One of the main feature of FD-MIMO systems distinct from the MIMO systems of the current LTE and LTE-Advanced standards is to employ a large number of antennas at eNB. In theory, as the number of eNB antennas N_T increases, cross-correlation of two random channel realizations goes to zero [1]. As a result, the interuser interference in the downlink can be controlled via a simple linear precoder and multiuser interference in the uplink can be eliminated via a simple receive combiner. Such benefit, however, can be realized only when the perfect CSI is available at the eNB. While the CSI acquisition in time division duplex (TDD) systems is relatively simple due to the channel reciprocity, such is not the case for frequency division duplex (FDD) systems. Basically, time variation and frequency response of channel is measured in FDD systems via the donwlink RSs and then sent back to the eNB after the quantization. Even in TDD mode, one cannot solely rely on the channel reciprocity because the measurement at the transmitter does not capture the downlink interference from neighboring cells or co-scheduled UEs. As such, downlink RSs are still required to capture channel quality indicator (CQI) for the TDD mode and thus the downlink RSs transmission and the uplink CSI feedback are essential for both duplex modes. Identifying the potential issues of CSI acquisition and developing the proper solutions is, therefore, of great importance for the successful commercialization of FD-MIMO systems. Two major problems related to the CSI acquisition process are as follows.

- **Degradation of CSI accuracy**: One well-known problems for the MIMO systems, in particular for FDD-based systems, is that the quality of CSI is affected by the limitation of feedback resources. As the CSI distortion increases, quality of the MU-MIMO precoder to control the interuser interference is degraded and so will be the performance of FD-MIMO systems [5]. In general, the amount of CSI feedback, determining the quality of CSI, needs to be scaled with N_T to control the quantization error so that the overhead of CSI feedback would be a concern in massive MIMO regime.
- **Increase of pilot overhead**: An important problem related to the large-scale antennas at eNB yet to be discussed separately is the pilot overhead problem. UE performs the channel estimation using the RS transmitted from the eNB. Since RSs need to be assigned in an orthogonal fashion, RS overhead typically grows linearly with N_T. For example, if $N_T = 64$,

approximately 48% of resource will be used for RS in LTE systems. Clearly, this overhead is undesirable since the RS eats out the downlink resources for the data transmission.

B. 2D active antenna system (AAS)

Another interesting feature of the FD-MIMO system is an introduction of the active antenna with 2D planar array. In the active antenna-based systems, gain and phase are controlled by the active components such as power amplifier (PA) and low noise amplifier (LNA) attached to each antenna element. In the 2D structured antenna array, one can control the radio wave on both vertical (elevation) and horizontal (azimuth) direction so that the control of the transmit beam in three dimension space is possible. This type of wave control mechanism is referred to as the *3D beamforming*. Another benefit of 2D planar array is that it can accommodate a large number of antennas without increasing the deployment space. For example, when 64 linear antenna arrays are deployed in a horizontal direction, under the common assumption that the antenna spacing is half wavelength ($\frac{\lambda}{2}$) and the system is using LTE carrier frequency (2 GHz), it requires a horizontal room of 3m. Due to the limited space on rooftop or mast, this space would be burdensome for most of cell sites. In contrast, when antennas are arranged in a square array, relatively small space is required (e.g., 1.0 $\times$ 0.5m with dual-polarized 8 $\times$ 8 antenna array).

C. 3D channel environment

When basic features of the FD-MIMO systems are provided, the next step is to design a system maximizing performance in terms of throughput, spectral efficiency, and peak data rate in the realistic channel environment. There are various issues to consider in the design of practical systems. Notable issues include investigation and characterization of the channel model of realistic deployment scenario for the performance evaluation. While the conventional MIMO systems consider the propagation in the horizontal direction only, FD-MIMO systems employing 2D planar array should consider the propagation in both vertical and horizontal direction. To do so, geometric structure of the transmitter antenna array and propagation effect of the three-dimensional positions between the eNB and UE should be reflected in the channel model. Main features of 3D channel propagation obtained from real measurement are as follows [7]:

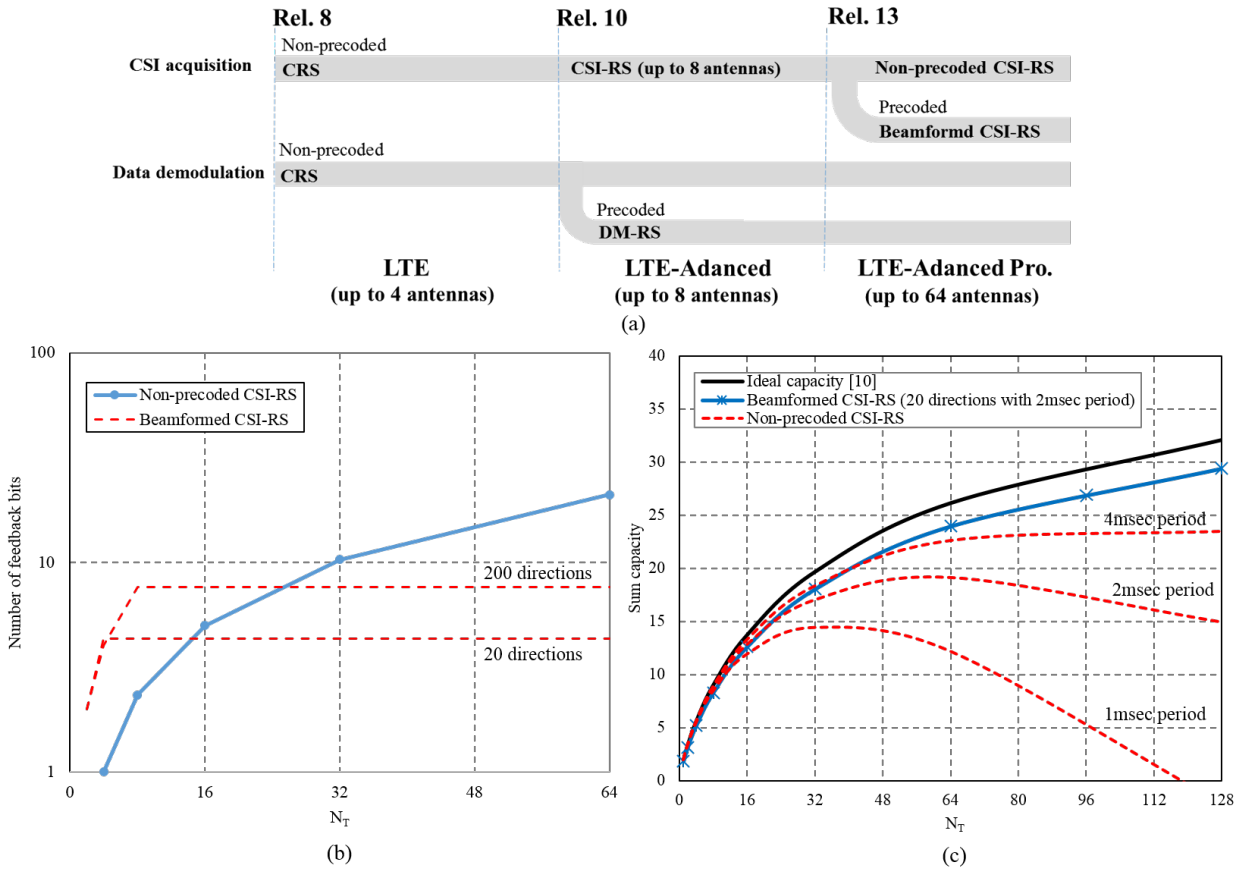

Fig. 1. MIMO evaluation: (a) RS evolution in LTE systems (b) Uplink feedback overhead (SNR=10dB [8]) (c) MU-MIMO capacity with considering CSI-RS overhead (Ideal CSI and ZFBF MU-precoding with 10 UEs and SNR=10dB [9]).

- Height and distance-dependent line-of-sight (LOS) channel condition: LOS probability between eNB and UE increases with the UE's height and also increases when the distance between eNB and UE decreases.
- Height-dependent pathloss: UE experiences less pathloss in higher floor (e.g., 0.6dB/m gain for macro cell and 0.3dB/m gain for micro cell).
- Height and distance-dependent elevation angular-spread of departure (ESD): when the location of eNB is higher than UE, ESD decreases with the height of UE (reflecting diffraction angles from above-rooftop propagation). It is also observed that the ESD decreases sharply as a UE moves away from the eNB.

D. RS transmission for CSI acquisition

From the Rel. 8 LTE to Rel. 12 LTE-Advanced, there has been substantial improvement in the RS scheme (See Fig. 1(a)). In the LTE system, common RS (CRS) has been exclusively used for channel training and data demodulation. In LTE-Advanced system, two new RSs, viz., channel state information RS (CSI-RS) and demodulation RS (DM-RS) have been introduced to perform the CSI acquisition and demodulation of data channel, respectively. While the CRS is transmitted with 1ms period, CSI-RS, used mainly for the CSI measurement in fixed or low-mobility scenarios, is transmitted with a multiple of 5ms period. While the CSI-RS is common to all users in a cell and thus un-precoded, the DM-RS is UE-specific (dedicated to each UE) so that it is precoded by the same weight applied for the data transmission. Since the DM-RS is present only on time/frequency resources where the UE is scheduled, this is not appropriate for CSI measurements [6].

One of the key features of the FD-MIMO systems distinct from previous LTE standards is to use a beamformed RS, called beamformed CSI-RS, for the CSI acquisition. Beamformed RS transmission is a technique that changes the radiation pattern of RS using the precoding weight. This scheme provides many benefits over non-precoded CSI-RS in the massive MIMO regime. Some of benefits are summarized as follows:

- **Less uplink feedback overhead:** In order to maintain a rate comparable to the case with perfect CSI, feedback bits, used for the channel vector quantization, should be proportional to the number of transmit antennas N_T [8]. Whereas, the amount of feedback for the beamformed CSI-RS scales logarithmic to the number of RSs ($\log_2 N_B$) since this scheme only feeds back an index of the best beamformed CSI-RS. Thus, as depicted in Fig. 1(b), benefit of beamformed CSI-RS is pronounced when N_T is large.
- **Less downlink pilot overhead:** When the non-precoded CSI-RS is used, pilot overhead increases with N_T, resulting in a substantial loss of the sum capacity in FD-MIMO regime (see Fig. 1(c)). Whereas, pilot overhead of the beamformed CSI-RS is proportional to N_B and independent of N_T so that the rate loss of the beamformed CSI-RS is marginal even when N_T increases.
- **Higher quality (SNR) in RS:** If the transmit power is P watt, P/N_T watt is used for each non-precoded CSI-RS transmission while P/N_B watt is used for the beamformed CSI-RS. For example, when $N_T = 32$ and $N_B = 12$, beamformed CSI-RS provides 4.3dB gain in

SNR over the non-precoded CSI-RS.[2]

In order to support the beamformed CSI-RS scheme, new transmitter architecture called transceiver unit (TXRU) architecture has been introduced. By TXRU architecture, we mean a hardware connection between the baseband signal path and antenna array elements. In the active antenna system, patch antennas and active devices are integrated on the printed circuit board (PCB) so that one can easily design paths between TXRUs and antenna elements. Since this architecture facilitates the control of phase and gain in both digital and analog domain, more accurate control of the beamforming direction is possible. One thing to note is that the conventional codebook cannot measure the CSI of the beamformed transmission so that new channel feedback mechanism supporting the beamformed transmission should be introduced (See Section III.D for details).

III. System Design and Standardization of FD-MIMO Systems

The main purpose of Rel. 13 study item is to identify key issues to support up to 64 transmit antennas placed in form of 2D antenna array. Standardization of the systems supporting up to 16 antennas is an initial target of Rel. 13 and issues to support more than 16 antennas will be discussed in subsequent releases. In the study item phase, there has been extensive discussion to support 2D array antennas, elaborated TXRUs, enhanced channel measurement and feedback schemes, and also increased number of co-scheduled users (up to 8 users). Among these, an item tightly coupled to the standardization is the CSI measurement and feedback mechanism. In this subsection, we discuss the deployment scenarios, TXRU structure, new RS strategy and corresponding feedback mechanism.

A. Deployment scenarios

For the design and evaluation of FD-MIMO systems, a realistic scenario where antenna array and UEs are located in different height are considered. To this end, two typical deployment scenarios, viz., 3D urban macro scenario (3D-UMa) and 3D urban micro (3D-UMi), are introduced (see Fig. 2). In the former case, transmit antennas are placed over the rooftop and in the latter case, those are located below the rooftop. In case of 3D-UMa, diffraction over the rooftop is a dominant factor for the propagation so that down-tilted transmission in the vertical direction

[2]In 3D channel model, the typical number of multi-paths (clusters) is 12 [7].

is desirable. In fact, by transmitting beams with different steering angles, eNB can separate channels corresponding to multiple UEs. In the 3D-UMi scenario, on the other hand, location of users is higher than the height of antenna so that direct signal path is dominant. In this scenario, both up and down-tilting are needed to schedule UEs in different floors. Since the cell radius of the 3D-UMi scenario is typically smaller than that of 3D-UMa, LOS channel condition is predominant so that more UEs can be co-scheduled without increasing the interuser interference [7]. Although not as strong as 3D-UMi scenario, LOS probability in 3D-UMa scenario also increases when the distance between eNB and UE decreases.

B. Antenna configurations

Unlike the conventional MIMO systems relying on the passive antenna, systems based on the active antenna can dynamically control the gain of an antenna element by applying the weight to low-power amplifiers attached to each antenna element. Since the radiation pattern depends on the antenna arrangement such as the number of the antenna elements and antenna spacing, the antenna system should be modeled in an element-level. As shown in Fig. 3(a), there are three key parameters characterizing the antenna array structure (M, N, P): the number of elements M in vertical direction, the number of elements N in horizontal direction, and the polarization degree P ($P = 1$ is for co-polarization and $P = 2$ is for dual-polarization). As a benchmark setting, 2D planar array using dual polarized antenna ($P = 2$) configuration with $M = 8$ (0.8λ spacing in vertical direction) and $N = 4$ (0.5λ spacing in horizontal direction) is suggested.[3] In this setting, null direction, an angle to make the magnitude of beam pattern to zero, for the elevation beam pattern is 11° and that for the horizontal beam pattern is 30° (see Fig. 3(c)). Since the null direction in the vertical domain is much smaller than that of the horizontal domain, scheduling UEs in the vertical domain is more effective in controlling the interuser interference. Note that tall or fat array structure ($M \gg N$ or $M \ll N$) is favorable since it will generate sharp beam but it might be less flexible in the situation where surrounding environment is changed. Also, large antenna spacing might be a desirable option but it can also increase inter-cell interference due to the coverage enhancement (caused by the effective SNR enhancement). For this reason, in a real deployment scenario, the design parameters should be carefully chosen by considering various factors such as user location, cell radius, building height, and antenna height.

[3]Note that the total number of antenna elements in this setup is the same as that of 8Tx antennas in conventional systems [10].

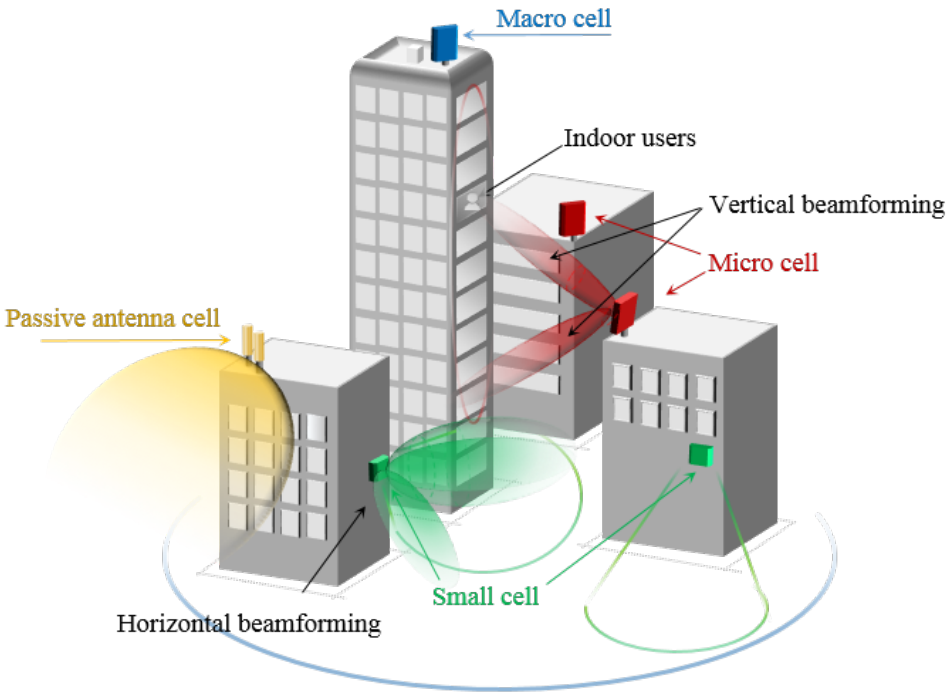

Fig. 2. FD-MIMO deployment scenarios; 3D macro cell site (placed over the rooftop) and 3D micro cell site (placed below the rooftop) with FD-MIMO small cells.

C. TXRU architectures

As mentioned, one interesting feature of the active antenna systems is that each TXRU contains PA and LNA so that eNB can control the gain and phase of an individual antenna element. In order to support this, a power feeding network between TXRUs and antenna elements called *TXRU architecture* is introduced [11]. TXRU architecture consists of three components: TXRU array, antenna array, and radio distribution networks (RDN). A role of the RDN is to deliver the transmit signal from PA to antenna array elements and received signals from antenna array to LNA. Depending on the CSI-RS transmission strategy, two representative options, *array partitioning* and *array connected architecture*, are suggested. In the array partitioning architecture, antenna elements are divided into multiple groups and each TXRU is connected to one of them (see Fig. 3(d)). Whereas, in the array connected structure, RDN is designed such that RF signals of multiple TXRUs are delivered to the single antenna element. To mix RF signals from multiple TXRUs, additional RF combining circuitry is needed as shown in Fig. 3(e). The difference between two can be better understood when we discuss the transmission of the CSI-RS. In the array partitioning architecture, N_T antenna elements are partitioned into L groups of

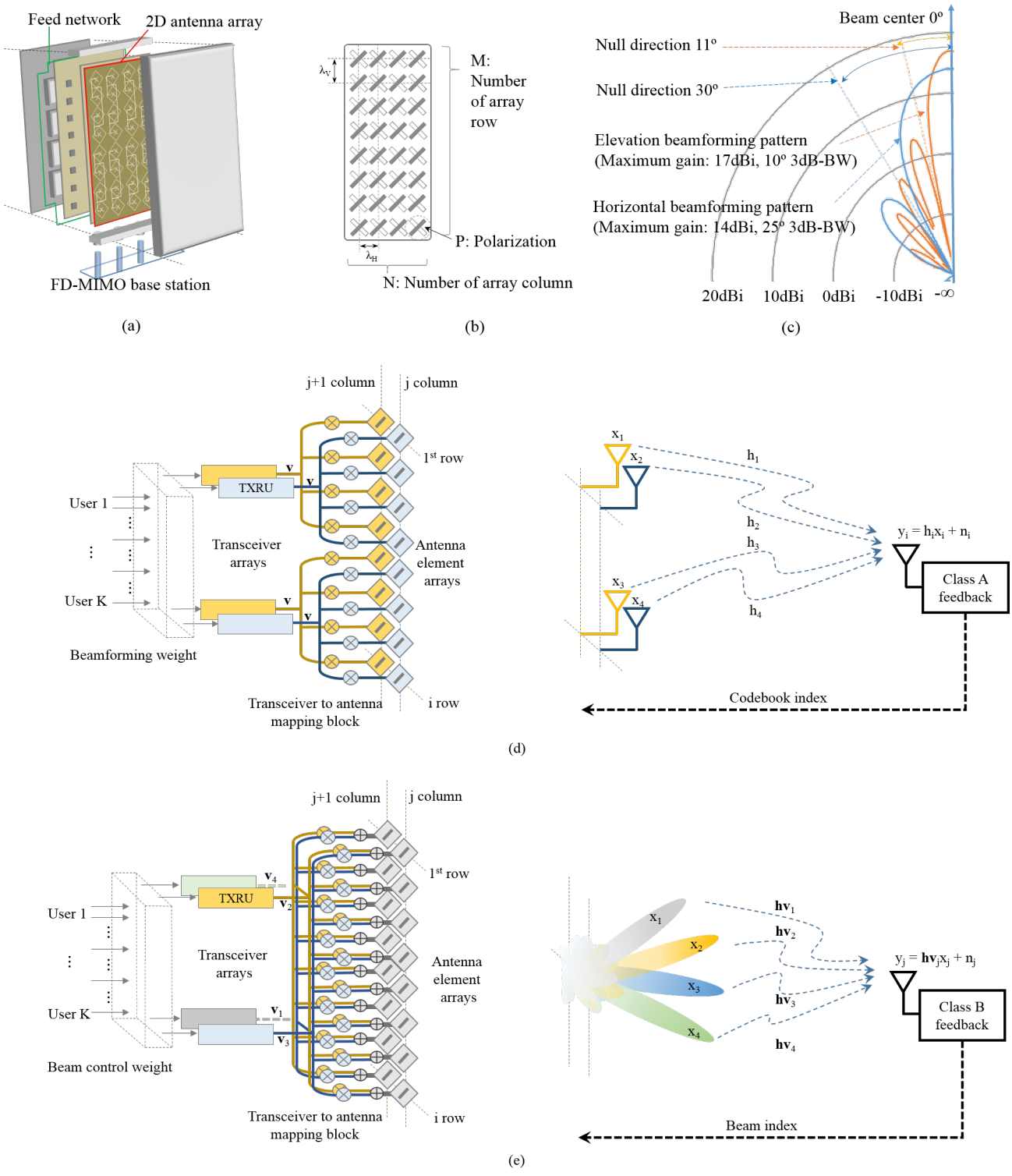

Fig. 3. FD-MIMO systems: (a) concept of FD-MIMO systems, (b) 2D array antenna configuration, (c) vertical and horizontal beamforming patterns, (d) array partitioning architecture with the conventional CSI-RS transmission, and (e) array connected architecture with beamformed CSI-RS transmission.

TXRU and orthogonal CSI-RS is assigned for each group. Each TXRU transmits its own CSI-RS so that the UE should measure the channel h from the non-precoded CSI-RS observation $y = hx+n$ of all TXRUs. In the array connected architecture, each antenna element is connected to $L^{'}$ (out of L) TXRUs and orthogonal CSI-RS is assigned for each TXRU with $N_T\frac{L^{'}}{L} = N_c$ dimension weight vector (see Fig. 3(e) for $L^{'} = L$ and $N_c = N_T$). Letting $\mathbf{h} \in \mathbb{C}^{1\times N_c}$ be the channel vector and $\mathbf{v} \in \mathbb{C}^{N_c\times 1}$ be the precoding weight, UE measures the precoded channel $\mathbf{hv}$ from the beamformed CSI-RS observation $y = \mathbf{hv}x + n$. Due to the narrow and directional CSI-RS beam transmission with linear array, SNR of precoded channel is maximized at the target direction.[4]

D. New CSI-RS transmission strategy

In the FD-MIMO systems, two CSI-RS transmission strategies, i.e., extension of conventional non-precoded CSI-RS and beamformed CSI-RS, are suggested. In the first strategy, UE observes non-precoded CSI-RS transmitted from each of partitioned antenna arrays (see Fig.3(d)). By choosing the precoder maximizing the properly designed performance criterion, UE can adapt to the channel variation. In the second strategy, eNB transmits multiple beamformed CSI-RS (for simplicity, we call it *beam*) using connected arrays architecture. Among these, UE selects the preferred beam and then feeds back its index. When eNB receives the beam index, the weight corresponding to the selected beam is used for data transmission. In doing so, eNB obtains the channel direction information.

Overall downlink precoder for data transmission $\mathbf{W}_{\text{data}}$ can be expressed as

$$\mathbf{W}_{\text{data}} = \mathbf{W}_T\mathbf{W}_P\mathbf{W}_U \tag{1}$$

where $\mathbf{W}_T \in \mathbb{C}^{N_T\times L}$ is the precoder between TXRU to antenna element, and $\mathbf{W}_P \in \mathbb{C}^{L\times N_P}$ is the precoder between CSI-RS port to TXRU (N_P is the number of antenna ports), and $\mathbf{W}_U \in \mathbb{C}^{N_P\times r}$ is the precoder between data channel to CSI-RS port. Note that the weight applied to the CSI-RS is the product of $\mathbf{W}_T$ and $\mathbf{W}_P$ while the weight applied to the data transmission is the product of $\mathbf{W}_T$, $\mathbf{W}_P$, and $\mathbf{W}_U$. In the following, we summarize details of two strategies.

- Conventional CSI-RS transmission: One simple option to maximize the benefit of precoding feedback is to do one-to-one mapping of the TXRU and the CSI-RS resource (i.e., $\mathbf{W}_P =$

[4]SNR $= \frac{|\mathbf{hv}(\phi)|^2}{\sigma^2}$, where ϕ is the beam direction and σ^2 is the noise power.

$\mathbf{I}_{N_{TXRU}}$). To achieve the same coverage between CSI-RSs, an identical weight $\mathbf{v}$ is applied to L groups.[5] Each UE measures the CSI-RS resources and then chooses the preferred codebook index i^* maximizing the channel gain for each subband:

$$i^* = \arg\max_i \|\bar{\mathbf{h}}^H \mathbf{W}_U^i\|_2^2. \tag{2}$$

where $\|\mathbf{a}\|_2 = \sqrt{\sum_i |a_i|^2}$ and $\bar{\mathbf{h}} = \mathbf{h}/\|\mathbf{h}\|$ is the channel direction vector, and $\mathbf{W}_U^i$ is the ith precoder between data channel and CSI-RS ports. This mechanism is called class A CSI feedback.

- Beamformed CSI-RS transmission: In order to obtain the spatial direction of UEs, eNB transmits multiple beamformed CSI-RSs. Let N_B be the number of CSI-RS, then we have $\mathbf{W}_T = [\mathbf{v}_1 \mathbf{v}_2 \dots \mathbf{v}_{N_B}]$ where $\mathbf{v}_i \in \mathbb{C}^{N_T \times 1}$ is the 3D beamforming weight for the ith beam. For example, when the rank-1 beamforming is applied, we have $\mathbf{W}_P = \mathbf{1}_{N_B}$ and $\mathbf{W}_U = 1$. Among all possible beams $\mathbf{v}_1, ..., \mathbf{v}_{N_B}$, UE selects and feeds back the best beam index j^* maximizing the received power:

$$j^* = \arg\max_j |\bar{\mathbf{h}}^H \mathbf{v}_j|^2. \tag{3}$$

This beam based mechanism is called class B CSI feedback. Under the rich scattering environment, dominant paths between eNB and UE depend on the direction and width of the transmit signal. In the MISO channel, for example, the channel vector in angular domain is expressed as $\mathbf{h} = \sum_i e_r \mathbf{e}_t(\phi_i)^*$, where $e_r = 1$ and $\mathbf{e}_t(\phi_i) = [1 \ ... \ \exp(-j2\pi(N_T - 1)\gamma\phi_i)]^T$ is the spatial signature of the transmitter (ϕ_i is direction of ith path and γ is normalized antenna spacing) [13]. When the RS is transmitted in a direction ϕ_j, the beamforming weight would be $\mathbf{v} = \mathbf{e}_t(\phi_j)$ so that the resulting beamformed channel is readily expressed as a one or at most a few dominant taps ($\mathbf{e}_t(\phi_i)^T \mathbf{e}_t(\phi_i) \approx 0$ when $i \neq j$). In fact, by controlling the weight applied to CSI-RS, effective dimension of the channel vector can be reduced and hence one can reduce the feedback overhead substantially.

In Table I, we summarize the CSI-RS transmission schemes discussed in the FD-MIMO.

E. CSI Feedback Mechanisms for FD-MIMO Systems

In the study item phase, various RS transmission and feedback schemes have been proposed. As shown in Fig. 1, capacity and overhead of class A and B feedback schemes are more or less

[5]In this paper, we assume that discrete Fourier transform (DFT) weights are used as $\mathbf{W}_T$ for mapping between TXRU and antenna elements for simplicity. For example, $\mathbf{W}_T$ can be expressed as $\mathbf{W}_T = [\mathbf{v} \ \mathbf{v}; \mathbf{v} \ \mathbf{v}]$ in Fig. 3(d).

TABLE I

COMPARISON BETWEEN CSI-RS TRANSMISSION AND CSI FEEDBACK CLASSES

Category	Class A CSI feedback (Conventional CSI-RS)	Class B CSI feedback (Beamformed CSI-RS)
Feedback design	Need to design codebook for 2D antenna layout and feedback mechanism for adapting channel variation	Need to devise a method to feed back beam index for adapting both weight changes and channel variation
UL Feedback overhead	Depend on resolution of codebook and the number of antennas	Depend on the number of operating beam N_B
CSI-RS overhead	Require N_T CSI-RS resources	Scale linearly with the number of beam N_B
Backward compatibility	Supportable with virtualization between TXRUs and antenna ports	Supportable with vertical 1D beamforming weight
Forward compatibility	Scalable to larger TXRU system if CSI-RS resources are allowed	Scalable to larger TXRU system if long-term channel statistics are acquired

similar in the initial target range (10 and 20 antennas) so that Rel.13 has decided to support both classes. In this subsection, we briefly describe codebook, RS transmission, CSI feedback schemes discuss in the standardization. Among various schemes, composite codebook and beam index feedback have received much attention as a main ingredients for class A and B CSI feedback. Rest will be considered in the future release.

Composite codebook: In this scheme, overall codebook is divided into two (vertical and horizontal codebooks) and thus the channel information is separately delivered to eNB. By combining two codebooks (e.g., Kronecker product of two codebooks $\mathbf{W}_U = \mathbf{W}_{U,V} \otimes \mathbf{W}_{U,H}$), eNB reconstructs whole channel information. Considering that the angular spread of the vertical direction is smaller than that of the horizontal direction, one can reduce the feedback overhead by setting relatively long reporting period to the vertical codebook. The conventional LTE codebook can be reused for horizontal codebook, but it might be better to newly design the vertical codebook to achieve better tradeoff between performance and feedback overhead.

Beam index feedback: To obtain the UE's channel direction information (CDI) from beamformed CSI-RSs, eNB needs to transmit multiple beamformed CSI-RSs. When the channel rank is one, feedback of a beam index and corresponding CQI is enough. Whereas, when the channel rank is two, co-phase information is additionally required for dual-polarized antennas. For example, once eNB obtains the CDI, this can be used for the beamforming vector of two-port CSI-RS and each CSI-RS port is mapped to the different polarized antennas. UE then estimates

and feeds back short-term co-phase information between two ports. A drawback of this scheme is that a large number of beams are needed to obtain an accurate CDI.

Partial CSI-RS with dimensional feedbacks: When we use the conventional feedback scheme, under the same CSI-RS density requirement (1 RE/port/RB pair), CSI-RS overhead will increase with the number of TXRUs. One simple yet effective approach for reducing the overhead is to use only subset of antennas for the CSI measurement. For example, by partitioning the 2D antenna array into horizontal and vertical ports, says N_H ports in the row and N_V ports in the column, the total number of CSI-RS can be reduced from $N_H \times N_V$ to $N_H + N_V$. This scheme, dubbed as partial CSI-RS transmission, can be easily mapped into a single RB without changing the current CSI-RS density. Overall channel information can be reconstructed by exploiting spatial and temporal correlation among antenna elements [14].

Adaptive CSI feedback with class A and B: The purpose of this feedback scheme is to collect benefits of the beamformed and conventional (non-precoded) CSI-RS transmission simultaneously. First, in order to acquire long-term channel information, eNB transmits N_T non-precoded CSI-RSs. After receiving sufficient long-term channel statistics from UE, eNB generates and then transmits the beamformed CSI-RSs which are used for short-term and subband feedbacks. For example, channel dimension of the beamformed CSI-RS can be reduced by projecting full dimensional channel information into the dominant eigen-directions of long-term channel information. In doing so, short-term feedback overhead can be reduced substantially. Also, long-term feedback overhead can be reduced by transmitting the conventional CSI-RS with a long duty cycle.

Flexible/Configurable codebook: In order to support various 2D antenna layouts without increasing the number of codebooks, flexible codebook scheme can be employed. In this approach, one master codebook is designed for a large number of TXRUs, say 16 TXRUs, and the specific codebook (e.g., (2×8), (4×4), or (1×16)) is derived based on this. To support this, the eNB needs to send the layout information via separate signaling and UE reconstructs the actual codebook using this information. To achieve further improvement in performance, one can additionally control the codebook resolution based on the user distribution. For example, when the antenna is placed in front of high-rise building, the eNB can assign more quantization bits to the vertical direction such that the vertical direction has better resolution than the horizontal direction.

IV. Performance of FD-MIMO System

In order to observe the potential gain of the FD-MIMO systems, we perform system-level simulations under the realistic multicell environment. In our simulations, we test two typical deployment scenarios (3D-UMa and 3D-UMi) with 2-tier hexagonal layout. As a performance metric, we use spectral efficiency for cell average and cell edge. Detailed simulation parameters are provided in Table II. We first investigate the system performance of FD-MIMO systems with two types of antenna configuration. For type I and II configurations, $(M, N, P) = (8, 4, 2)$ and $(M, N, P) = (32, 4, 2)$ are used, respectively. In the type II configuration, antenna spacing is set to four times larger than the spacing of type I. To investigate the effect of antenna structure, ideal feedback under full buffer traffic model (each user has unlimited amount of data to transmit) is used. In Fig. 4(a), we plot the throughput of the conventional LTE systems with 8Tx ($N_V \times N_H = 1 \times 8$) and FD-MIMO systems with 16, 32, and 64Tx ($N_V \times N_H = 2 \times 8,\ 4 \times 8,$ and 8×8) where N_V and N_H are the number of CSI-RS in vertical and horizontal dimension, respectively. This results shows that both antenna configuration provide large gain over the conventional 8Tx in LTE-A, resulting in 105% (type I) and 484% (type II) gain at cell edge, respectively. Due to the sufficient antenna spacing, cross-correlation between channels becomes negligible, and thus the spectral efficiency of type II increases linearly with the TXRU, resulting in 30% (cell average) and 70% gain (cell edge) when the number of TXRUs is doubled [15]. However, due to the insufficient antenna spacing, the spectral efficiency of type I configuration does not scale linearly with the number of TXRUs.

We next investigate the system performance of FD-MIMO system under finite traffic model (e.g., FTP model) where each UE with distinct arrival time receives a file with finite size. As a performance metric, we use a user packet throughput (number of successively received packet during the transmission period). In order to support backward compatibility and also perform fair comparison among schemes under test, we employ the conventional MMSE based channel estimation. In our simulations, following CSI feedback strategies are considered.

- **Conventional 8Tx LTE Systems**: 8Tx codebook based on Rel.10 LTE-A feedback mechanism is used. The implicit feedback is used for the CSI feedback.
- **FD-MIMO systems with**
  - **Non-precoded CSI-RS**: Composite codebook of horizontal and vertical codebooks is used. In case of 16Tx with ($N_V \times N_H$=2 $\times$ 8) antenna configuration, the codebook is

generated via the Kronecker product of 2Tx and 8Tx LTE codebooks. The implicit feedback (RI, horizontal and vertical PMIs, CQI) is used for the CSI feedback.

- **Beamformed CSI-RS scheme I**: Beam index feedback is used. Vertical coverage angle is represented by 4 fixed distinct beams ($N_B = 4$). Each UE reports the best beam index (BI) and corresponding CQI.
- **Beamformed CSI-RS scheme II**: The eNB transmits both non-precoded CSI-RS and beamformed CSI-RS. UE feeds back long-term CSI (RI, long-term PMI) using the non-precoded CSI-RSs and also reports short-term CSI (BI, CQI) using the beamformed CSI-RSs ($N_B = 4$). Note that the eNB keeps changing the precoding weight of beamformed CSI-RS using long-term PMI.

In Fig. 4(c), we plot the user throughput of the finite traffic model as a function of packet arrival rate. Note that when the packet arrival rate is high, co-scheduled users increase and thus intercell and multiuser interference will also increase. In this realistic scenario, FD-MIMO systems outperform the conventional MIMO systems with a large margin, achieving 1.5× and 3× improvement in performance in cell average and edge user packet throughput, respectively. Note that in the low network loading (low interference scenario), gain of the FD-MIMO systems is coming from the 3D beamforming and in the medium to high network loading (high interference scenario), gain is mainly due to the multiuser precoding of the 2D active antenna array. Fig. 4(d) summarizes the throughput of various CSI feedback frameworks. With the same feedback overhead (2bit), beamformed CSI-RS scheme I outperforms non-precoded scheme with a large margin. This is because the number of the codebook for the channel feedback is only 4, so that channel state information at eNB is very poor. Since the beamformed CSI-RS scheme II can adapt weights of beamformed CSI-RS to generate an accurate CDI, it performs better than other schemes. It is worth mentioning that the non-precoded CSI-RS scheme requires a large amount of feedback overhead (approximately 128 quantization levels) to achieve comparable performance. From this observation, we clearly see that the beamformed CSI-RS transmission is effective in controlling the precoding weights (in time, frequency, and space), feedback overhead, and pilot resource overhead, and we expect that this scheme would be a key ingredient for future release of FD-MIMO.

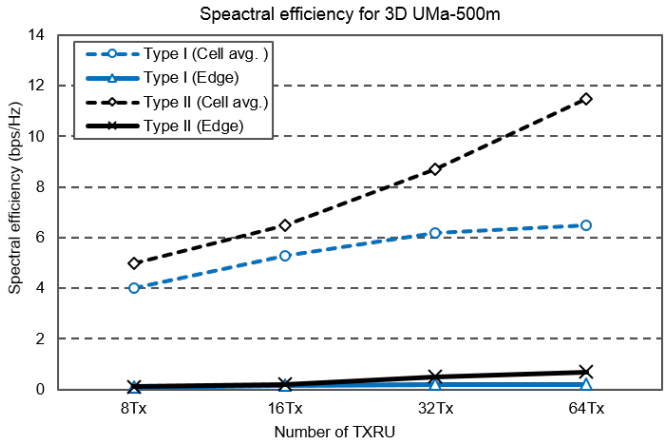

Full Queue Results (3D UMa-500m)			
	8TXRUs	64TXRUs (Type I)	64TXRUs (Type II)
Cell Avg. SE Gain	1X	1.62X	2.3X
Edge SE Gain	1X	2.05 X	5.84X

FTP Traffic Results (λ=3, 3D Umi-200m, 2GHz, non-precoded)		
	8TXRUs (Conventional)	16TXURs (FD-MIMO)
Cell Avg. SE Gain	1X	1.64X
Edge SE Gain	1X	3.0X

(b)

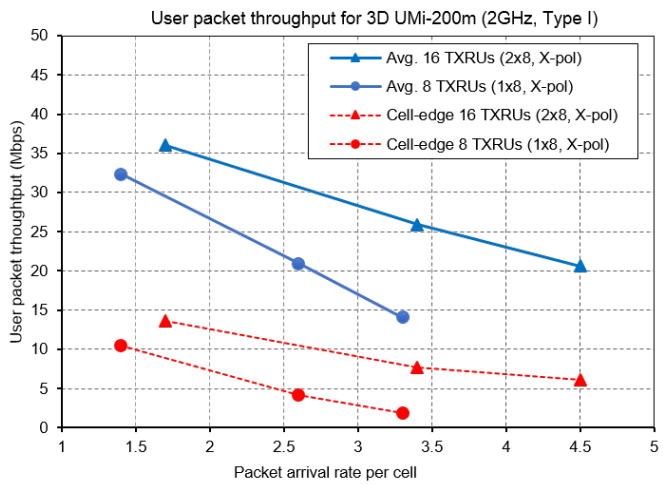

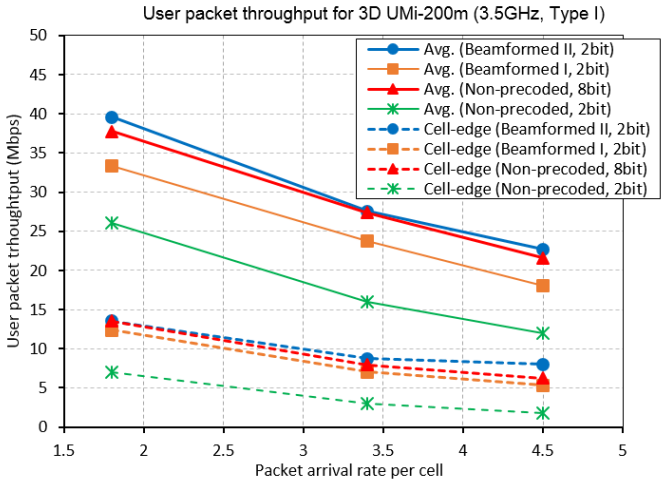

Fig. 4. System level performance results and comparison with full buffer and FTP traffic model.

V. Concluding Remarks

In this article, we have provided an overview of FD-MIMO systems in 3GPP LTE (recently named as LTE-Advanced Pro) with emphasis on the discussion and debate conducted on the Rel. 13 phase. We discussed key features of FD-MIMO systems, main issues in standardization of system design such as channel model, transceiver architectures, pilot transmission and CSI feedback scheme. We also presented the system level simulation results to demonstrate the potential gain of FD-MIMO systems. To make the most of large number of eNB antennas in a cost and space effective manner, new key features, distinct from MIMO system in conventional LTE-A, should be introduced in both standard, system design, and transceiver implementation. These

include new transmitter architecture (array connected architecture), new RS transmission scheme (beamformed CSI-RS transmissions), and enhanced channel feedback (beam index feedback), and many more. Although our work focus on the standardization in Rel. 13, there are still many issues for the successful deployment of FD-MIMO systems in the future including pilot transmission and advanced channel estimation exploiting channel sparsity, beam adaptation and optimization, and RS overhead reduction for throughput enhancement.

TABLE II

SYSTEM SIMULATION ASSUMPTIONS

Parameter	**Value**
Duplex method	FDD
Bandwidth	10 MHz
Center frequency	2GHz / 3.5GHz
Inter-site distance	500m for 3D-UMa, 200m for 3D-UMi
Network synchronization	Synchronized
Cellular layout	3D Hexagonal grid, 19 eNBs, 3 cells per site
Users per cell	10 (Uniformly located in 3D space)
Downlink transmission scheme	$N_T \times 2$ MU-MIMO SLNR precoding with rank adaptation with 2 layer per UE
Downlink scheduler	Proportional Fair scheduling in the frequency and time domain.
Downlink link adaptation	CQI and PMI 5ms feedback period 6ms delay total (measurement in subframe n is used in subframe $n+6$) Quantized CQI, PMI feedback error: 0% MCSs based on LTE transport formats
Downlink HARQ	Maximum 3 re-transmissions, IR, no error on ACK/NACK, 8ms delay between re-transmissions
Downlink receiver type	MMSE : based on demodulation reference signal (DM-RS) of the serving cell [12]
Channel estimation	Non-ideal channel estimation on both CSI-RS and DM-RS
Antenna configuration	$(M, N, P) = (8, 4, 2)$
TXRU configuration ($N_H \times N_V$)	1×8, 2×8, 4×8, and 8×8 with X-pol (0.5λ, 0.8λ antenna spacing for vertical and horizontal)
Control channel overhead, Acknowledgments etc.	Control channel: 3 symbols in a subframe Overhead of DM-RS: 12 RE/RB/Subframe Overhead of CSI-RS: in maximum 16 REs of CSI-RS every 5ms per RB (This is, in 8 Tx antenna case, 8 REs/RB per 10ms) Overhead of CRS: 2-ports CRS
Channel model	3D urban macro and micro channel model [7] with 3km/h UE speed
Inter-cell interference modeling	57 intercell interference links are explicitly considered.
Max. number of layers	4
Traffic model	Full buffer and non-full buffer (FTP Model) with 0.5 MBytes packet and various arrival rate

REFERENCES

[1] T. L. Marzetta, "Non cooperative cellular wireless with unlimited numbers of base station antennas", *IEEE Trans. Wireless Commun.*, vol. 9, no. 11, pp.3590 -3600, 2010

[2] Y. Kim, H. Ji, J. Lee, Y.H. Nam, B.L. Ng, I. Tzanidis, Y. Li and J. Zhang, "Full Dimension MIMO (FD-MIMO): The Next Evolution of MIMO in LTE Systems," *Wireless Commun. Mag.*, vol. 21, issue 3, 2014

[3] Y. H. Nam, B. L. Ng, Y. Sayana, Y. Li, J. Zhang, Y. Kim and J. Lee, "Full-dimension MIMO (FD-MIMO) for next generation cellular technology," *IEEE Commun. Mag.*, vol. 51, issue 6, 2014

[4] W. Zhang, J. Xiang, Y.R. Li, Y. Wang, Y. Chen, P. Geng and Z. Lu, "Field Trial and Future Enhancements for TDD Massive MIMO Networks," in *Proc. on 26th Intl. Symp. on Personal, Indoor, and Mobile Radio Comm. (PIMRC) Workshop Advancements in Massive MIMO*, 2015, pp. 1114-1118

[5] M. Sadek, A. Tarighat, and A. Sayed, "A leakage based precoding scheme for downlink multi user MIMO channels," *IEEE Trans. Wireless Commun.*, vol. 6, no. 5, pp. 1711-1721, 2007.

[6] C. Lim, T. Yoo, B. Clerckx, , B. Lee and B. Shim, "Recent trends in MU-MIMO,", *IEEE Commun. Mag.*, vol. 51, issue 3, 2014.

[7] 3GPP Technical Reports TR36.873, "Study on 3D channel model for LTE".

[8] N. Jindal, "MIMO broadcast channels with finite-rate feedback." *IEEE Trans. on Information Theory*, vol. 52, issue 11, 2006.

[9] T. Yoo, and A. Goldsmith, "Optimality of zero-forcing beamforming with multiuser diversity." , *IEEE Journal on Selected Areas in Comm.*, vol. 24, issue 3, 2006.

[10] 3GPP Technical Reports TR36.897, "Study on Elevation Beamforming/Full-Dimension (FD) MIMO for LTE".

[11] 3GPP Technical Reports TR36.847, "E-UTRA and UTRA; Radio Frequency (RF) requirement background for Active Antenna System (AAS) Base Station (BS)".

[12] E. Dahlman, S. Parkvall and J. Skold, 4G LTE/LTE-Advanced for Mobile Broadcast. Academia Press, 2011.

[13] D. Tae, and P. Viswanath, Wireless Communication. Cambridge University Press, 2005.

[14] B. Lee, J. Choi, J. Seol, D. Love, and B. Shim, "Antenna grouping based feedback compression for FDD-based massive MIMO systems", *IEEE Trans. on Commun.*, vol. 63, no. 9, pp. 3261-3274, Sept. 2015.

[15] G. D. Durgin and T. S. Rappaport, "Effects of multipath angular spread on the spatial cross-correlation of received voltage envelopes ", *IEEE Vehicular Techonlogy Conf.*, vol. 2, pp. 996-1000, Jul. 1999.